

Undulator Induced Resonances

J. Harris, P. Morton, J. Spencer, H. Winick
 Stanford Linear Accelerator Center
 Stanford University, Stanford, California 94305

Abstract

Undulators appear to be nearly ideal radiation sources for use in storage rings because of their high brightness and small perturbation on stored beam characteristics. We consider the effects of higher-order magnetic field errors and show how they increase beam size and may lead to unstable growth of betatron oscillations. We have observed such effects in SPEAR at betatron tunes satisfying the equations

$$3\nu_x + \nu_y = 21 \quad \text{and} \quad \nu_x + 3\nu_y = 21.$$

The widths of these resonances were measured to be $\Gamma = 0.008 \pm 0.004$. They are clearly visible on the synchrotron light monitors with a very dramatic and characteristic beam blow-up pattern (reminiscent of a Miller beer label). A model is developed which predicts the locations of the resonances, their widths and the projected shapes observed on the light monitors. By inducing such high-order coupling resonances one could study such things as the beam distribution in electron rings or possibly turbulent motion in proton rings.

I. Introduction

The effects of wigglers on stored particle beams have been considered in a number of review articles and conferences (e.g. see 1,2,3). Such things as energy broadening or transverse tune changes are seen to be rather modest and easily compensated for the insertions now going into existing rings. In fact, these effects can prove useful in unfolding the natural widths of particle resonances in high energy physics experiments (4) or determining the beta function at the wiggler (5). Here we consider the effects of possible higher order magnetic field errors associated with these devices. Because these errors tend to increase the beam cross section and can easily cause beam loss at the resonant tunes associated with the nonlinearity, it is important to know where such resonances occur and the relationship between the magnitude of the field errors and the widths of the resonances. Once again, such effects could prove serendipitous if one knows the error fields sufficiently well.

Our interest in this subject was stimulated by an effect observed in SPEAR when the first permanent magnetic undulator was installed. There was an occasional beam blow-up associated with the undulator which was subsequently shown to be associated with a $3\nu_x + \nu_y$ resonance which was quite close to the normal SPEAR operating point ($\nu_x = 5.273, \nu_y = 5.162$). This resonance was narrow (FWHM < 0.010) and easily observable on the light monitors (LM) whenever the peak field in the undulator was 1 kG or so. If such a resonance resulted from a rotated octupole field, then one also expects a $3\nu_y + \nu_x$ resonance which was also observed and which had a comparable blow-up pattern on the light monitor.

The undulator (6) has 30 periods with $\lambda \simeq 6$ cm. Each period has 4 rows of SmCo_5 blocks magnetized in directions changing by 90° from one row to the next. The blocks are 1.5 cm \times 1.5 cm in cross-section and 2.5 cm long with a remanent field $B_r = 8.1$ kG. Three blocks make up a row which is 7.5 cm long and perpendicular to the beam direction. The magnet gap is remotely adjustable from a minimum of about 3 cm to 6 cm, corresponding to a field varying from 2.4 kG to 0.5 kG and a K value varying from 1.37 to 0.28. Rotatable assemblies of magnet blocks are located at each end of the magnet to null the field integral so as to produce no net deflection of the electron beam on passing through the device.

II. Discussion

Because the undulator is located in a symmetry straight section of SPEAR, the betatron wavelengths ($\beta_x = 13.4$ and $\beta_y = 4.8$ m) are both sufficiently long and constant over the length of the undulator to allow us to consider any field perturbation (A_θ) as localized at its center. The tune dependence of the resonances clearly in-

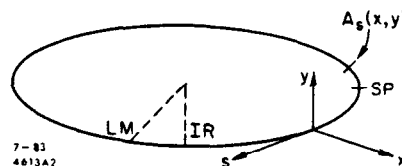


Fig. 1. Schematic of SPEAR and coordinate layout.

* Work supported by the Department of Energy, contract DE-AC03-76SF00515.

dicating the existence of a field with octupole symmetry. One may then ask whether it is possible to predict the important characteristics observed in terms of a linear ring model with nonlinear perturbations? The situation is shown schematically in Fig. 1 which shows the locations of the interaction region, light monitor and undulator.

The equations for the betatron motion in this storage ring, ignoring damping, can then be written as

$$\frac{d^2x}{d\theta^2} + K_x^2(\theta)x = -\frac{\lambda R}{B\rho}\delta(\theta)[3x^2y - y^3]$$

$$\frac{d^2y}{d\theta^2} + K_y^2(\theta)y = \frac{\lambda R}{B\rho}\delta(\theta)[3y^2x - x^3] \quad (1)$$

where we have used $\theta = s/R$ as the independent coordinate. K_x and K_y represent the quadrupole focusing, R is the average ring radius, $B\rho$ the magnetic rigidity of the electron and λ is the integral field strength (kG-m/m³). These equations are derivable from the Hamiltonian:

$$H_0 = \frac{p_x^2}{2} + \frac{p_y^2}{2} + K_x^2(\theta)\frac{x^2}{2} + K_y^2(\theta)\frac{y^2}{2} + \frac{\lambda R}{B\rho}\delta(\theta)[x^3y - xy^3]. \quad (2)$$

We make the usual transformation (see Appendix) to action angle variables where

$$x = \sqrt{\frac{2\beta_x J_x}{R}} \cos[\psi_x + \int (R/\beta_x - \nu_x) d\theta] \quad (3)$$

with a similar expression used for y . We will ignore all terms in the new Hamiltonian that oscillate rapidly. When $(3\nu_x + \nu_y - m) \approx 0$ the quantity $\Psi = (3\psi_x + \psi_y - m\theta)$ is slowly varying and must be retained. The new Hamiltonian may then be written as

$$H = \nu_x J_x + \nu_y J_y + A J_x^{3/2} J_y^{1/2} \cos\Psi \quad (4)$$

where

$$A = \frac{\lambda \beta_x^{3/2} \beta_y^{1/2}}{4\pi R(B\rho)} \quad (5)$$

with β_x and β_y evaluated at the perturbation.

Using the equations of motion, which may be derived from the Hamiltonian in Eq. 4, we obtain the following two constants of the motion

$$K_1 = J_x - 3J_y \quad (6)$$

and

$$K_2 = \epsilon J_y + A J_x^{3/2} J_y^{1/2} \cos\Psi \quad (7)$$

with

$$\epsilon = (3\nu_x + \nu_y - m). \quad (8)$$

We will consider the case where the initial value of the y motion is zero ($J_y = J_{y0} = 0$) and $J_x = J_{x0} \neq 0$. Equations 6 and 7 may be rewritten as

$$J_y = \frac{1}{3}(J_x - J_{x0}) \quad (9)$$

and

$$J_y^{1/2} = \left(\frac{-A \cos\Psi}{\epsilon} \right) J_x^{3/2}. \quad (10)$$

Since we must have both J_x and J_y positive, the sign of $\cos\Psi$ must be opposite to the sign of ϵ . Equation 10 represents a family of curves in the J_y, J_x plane for various values of $\cos\Psi$. The boundaries of this family are given by $\cos\Psi = 0$, i.e. $J_y = 0$, and by $\cos\Psi = -\text{sgn}(\epsilon)$, i.e.

$$J_y = \left(\frac{A}{\epsilon} \right)^2 J_x^3. \quad (11)$$

Eq. 11 is plotted in Fig. 2 for various values of $|A/\epsilon|$.

The motion of J_x and J_y occurs along the $3J_y = (J_x - J_{x0})$ line (dotted in Fig. 2) between the point ($J_x = J_{x0}, J_y = 0$) and the intersection with the curve of Eq. 11. For large enough values of $|A/\epsilon|$ there is no intersection and both J_x and J_y may increase without limit. The maximum value of A/ϵ for stable motion is $J_{x0} = 2\epsilon/9A$.

If we substitute for J_x and A from equations 3 and 5 above, we find the condition for stability to be

$$\lambda \equiv \frac{B_{PT} \cdot L_u}{R_{PT}^3} \lesssim \frac{\pi(B\rho)\epsilon}{\beta_x^{1/2} \beta_y^{1/2} \langle x^2 \rangle}. \quad (12)$$

For SPEAR operation at 3 GeV, with the undulator, this implies a limit on the effective pole tip field at 1 cm radius of $B_{PT} \approx 1.5$ G for $\epsilon = 0.004$ and $\langle x^2 \rangle = (10\sigma_x)^2$. For the complimentary $3\nu_y + \nu_x - m = 0$ resonance one can substitute the corresponding y -aperture limit.

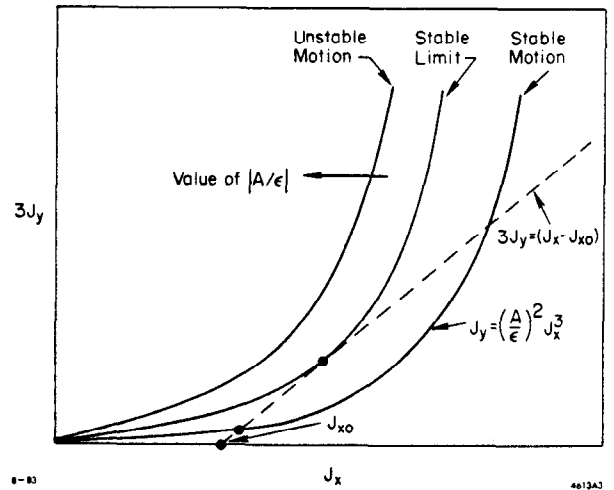


Fig. 2. Action variables showing stability regions.

III. Computer Simulations

To test the simple analytic theory, we have performed computer simulations of the particle motion in various approximations. We use a monochromatic, randomly generated distribution at the interaction region, based on a 4-dimensional, upright ellipse, defined by

$$\left(\frac{x}{\sigma_x}\right)^2 + \left(\frac{y}{\sigma_y}\right)^2 + \left(\frac{x'}{\sigma_{x'}}\right)^2 + \left(\frac{y'}{\sigma_{y'}}\right)^2 \equiv 1. \quad (13)$$

At 3 GeV and optimum coupling, the beam envelope at the IR is $(\sigma_x, \sigma_y) = (0.0760, 0.0057 \text{ cm})$ for a typical configuration with $(\beta_x^*, \beta_y^*) = (140, 10 \text{ cm})$. Fig. 3 shows a beam of 300 particles at both the IR and LM after only a few turns. Using an equivalent pole-tip field of 1 G at 1 cm for the octupole field we then propagate this distribution with the results shown in Fig. 3. The butterfly shape has the general form observed. Varying the tune by 0.004 shows virtually no change in the original, unperturbed envelope which then decreases when we include damping.

The time development of the beam profile is quite interesting and depends on both the rotation of the field, the field strength and the basic beam distribution used. A more quantitative way to study the beam profile using a weighted sample of elliptical shells and a color TV monitor is now being done.

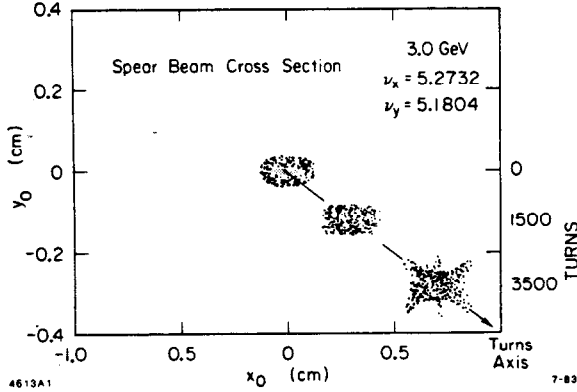


Fig. 3. Time development of resonance at LM in Fig. 1.

Appendix

We will demonstrate a method due to Symon, which eliminates the dependence of the Hamiltonian

$$H = \frac{p_x^2}{2} + K_x(\theta) \frac{x^2}{2} \quad (A1)$$

on the independent variable θ with the condition that $K_x(\theta + 2\pi) = K_x(\theta)$. The equation of motion that follows from this Hamiltonian is

$$x'' + \dot{K}_x(\theta)x = 0 \quad (A2)$$

and has two independent solutions $u_1(\theta)$ and $u_2(\theta)$ which we write in terms of the Floquet functions $\phi_x(\theta)$ and $\eta_x(\theta)$

$$\begin{aligned} u_1 &= \exp(i\nu_x \theta) \phi_x(\theta) & u_2 &= \exp(-i\nu_x \theta) \phi_x^*(\theta) \\ u_1' &= i \exp(i\nu_x \theta) \eta_x(\theta) & u_2' &= -i \exp(-i\nu_x \theta) \eta_x^*(\theta) \end{aligned}$$

We pick the Wronskian $(u_1 u_2' - u_1' u_2)$ equal to $(-4i)$ which gives

$$(\eta_x^* \phi_x + \eta_x \phi_x^*) = 4. \quad (A4)$$

Now we transform the Hamiltonian from coordinate (x, p_x) to (ψ_x, H_x) by the following generating function

$$F_3(p_x, \psi_x, \theta) = \frac{i}{2} p_x^2 \left[\frac{\phi_x \exp i\psi_x + \phi_x^* \exp -i\psi_x}{\eta_x \exp i\psi_x - \eta_x^* \exp -i\psi_x} \right] \quad (A5)$$

where

$$x = -\frac{\partial F_3}{\partial p_x}, \quad J_x = -\frac{\partial F_3}{\partial \psi_x} \quad (A6)$$

The results from Eq's. 6 and 7 give

$$H(J_x, \psi_x, \theta) = \nu_x J_x. \quad (A7)$$

We can, of course, do the same type of transformation for the vertical coordinates (y, p_y) to (ψ_y, J_y) . From Courant and Snyder we have the solution in terms of the betatron functions

$$u_1 = a \beta_x^{1/2}(\theta) \exp i \int^{\theta} \frac{R d\theta'}{\beta_x(\theta')} \quad (A8)$$

with

$$\nu = \frac{1}{2\pi} \int^{2\pi} \frac{R d\theta'}{\beta_x(\theta')}$$

When this is compared to our solutions u , we find that

$$\phi_x(\theta) = \sqrt{\frac{2\beta_x(\theta)}{R}} \exp i \int^{\theta} \left(\frac{R}{\beta_x(\theta')} - \nu \right) d\theta' \quad (A9)$$

References

1. Wiggler Magnets, ed. by H. Winick and T. Knight, SSRP Report 77/05 (1977).
2. Frascati Wiggler Meeting Proceedings, A. Luccio, A. Reale and S. Stipcich (eds), (1978).
3. J. Spencer and H. Winick, Chapter 21 in *Synchrotron Radiation Research* H. Winick and S. Doniach (eds), Plenum Press, New York, 1980.
4. M. Berndt, et al., IEEE Trans. Nucl. Sci. **26**, 3812-3815 (1979).
5. J. E. Spencer, *Wigglers - the Newest Profession*. SLAC-PUB-2677, 1981.
6. K. Halbach, J. Chin, E. Hoyer, H. Winick, R. Cronin, J. Yang and Y. Zambre, IEEE Trans. Nucl. Sci. **28**, 3136-38 (1981).